Nanoscale

PAPER

View Article Online
View Journal | View Issue

Cite this: *Nanoscale*, 2025, **17**, 8624

Self-healing and highly adhesive conductive polydimethylsiloxane-based elastomers for chronic epilepsy monitoring†

Miao Tang,[a] Ke Lei,[a] Xingying Zhao,[a] Xifeiling Hu,[a] Quansheng He,[a] Ke Zhang,[a] Xianhui Ma,[a] Hualiang Ni,[c] Yousheng Shu[a] and Zili Li *[b]

Flexible substrate materials with high adhesion, high stretchability, and low impedance are essential to ensure long-term stable acquisition of electrophysiological signals with less tissue inflammation. Polydimethylsiloxane is a promising candidate owing to its inherent flexibility and biocompatibility; however, its poor adhesion to the skin and excessive stiffness of tissue interfaces limit its application in this field. To address these challenges, we developed a flexible electrode system based on crosslinked block polyborosiloxane and carbon nanotube (C-PBS/CNT) elastomers carrying hydroxyl groups through a thiol–ene reaction. The composite exhibits enhanced adhesion to both the skin and skull, high stretchability, and tunable stiffness ranging from 10 to over 200 kPa, enabling adaptability to the long-term monitoring of epileptic activity and other application scenarios. Moreover, the C-PBS/CNT composite elastomer demonstrated excellent self-healing performance owing to its dynamic boronate ester and hydrogen bonds. The packaged C-PBS/CNT electrode demonstrates low impedance for efficient multi-channel acquisition of epileptic activity under humid conditions. These innovations enable a precise analysis of cortical epileptic-activity propagation and provide an essential technological platform for the prediction and treatment of epileptic seizures, paving the way for next-generation wearable biomedical devices.

Received 14th January 2025,
Accepted 24th February 2025

DOI: 10.1039/d5nr00171d

rsc.li/nanoscale

[a]*Jinshan Hospital, Institute for Translational Brain Science, Fudan University, Shanghai 200433, China*
[b]*School of Information Science and Technology, Fudan University, Shanghai, 200433, China. E-mail: lizili@fudan.edu.cn*
[c]*Aoyi Information Technology Co., Ltd, Shanghai 200433, China*

†Electronic supplementary information (ESI) available. See DOI: https://doi.org/10.1039/d5nr00171d

Zili Li

Dr Zili Li is currently an associate professor at the School of Information Science and Technology, Fudan University, China. He received his Ph.D. in polymer chemistry and physics from the University of Science and Technology of China. He was a postdoctoral fellow in Professor Zhiqun Lin's group at the Georgia Institute of Technology from 2018 to 2021. His research interests mainly focus on preparation of block and topological copolymers for directed self-assembly lithography, self-healing flexible electronics for health monitoring, and two-dimensional polymers for optoelectronic devices.

Introduction

Epilepsy is a chronic neurological disorder that affects approximately 50 million individuals globally with significant risks, such as trauma and sudden death during seizures.[1] The normal brain electrical activity is disrupted by the enhancement of the signal power within various frequency ranges during the preictal and ictal stages. Electrophysiological activities of neuron populations carry essential information about the mental state of people. Therefore, monitoring the electrical activities of the brain with electrodes is critical for the diagnosis and treatment of epilepsy and favorable for understanding the pathogenesis of diseases and supporting therapy.[2] Electroencephalography (EEG) and electrocardiogram (ECG) are two major techniques used to monitor brain activity and support the prognosis of epilepsy.[2,3] Neural electrodes are essential tools for epilepsy research, enabling the precise capture of neural electric signals and aiding the localization of epileptic foci. Many research groups have made a great effort to explain the mechanism and timing of seizures using various types of electrodes.[4–6] However, conventional neural electrodes are typically fabricated using rigid metals or semiconductor substrates. Their mechanical mismatch with soft brain tissues often leads to tissue damage, inflammation, and signal degradation, limiting their long-term clinical

applicability in epilepsy monitoring.[5] Moreover, the weak adhesion of conventional neural electrodes results in falling off from the skin or tissue during the occurrence of seizures with strenuous exercise.[7] These limitations highlight the urgent need for advanced substrate materials with flexibility, adhesion, and biocompatibility.

A polydimethylsiloxane (PDMS)-based electrode can mitigate this mechanical mismatch owing to its excellent flexibility and biocompatibility.[6–9] However, its intrinsic hydrophobicity and weak adhesion lead to delamination during seizure-induced movements, thereby compromising signal fidelity. High-energy treatment is an important strategy to introduce hydrophilic moieties on the PDMS substrate and enhance adhesive properties.[10–12] Nevertheless, the hydrophilic surface recovers its hydrophobicity upon contact with air.[10] An alternative strategy to create permanently hydrophilic PDMS and increase its adhesive properties is surface grafting with hydrophilic polymers[13–15] through surface oxidation treatment and subsequent chemical reactions. However, this modification process is time-consuming and tedious, and the structure of the resulting PDMS-based materials is uncontrollable. In addition, the chemical grafting process is usually implemented under organic solution conditions, limiting its application in biological samples. Therefore, it is urgent to prepare PDMS-based electrodes with controllability and high adhesive performance in the film state using convenient methods.

In addition, the PDMS elastomer is an intrinsic electrical insulating material, and incorporating conductive carbon nanotubes (CNTs) into polymer matrices is a promising strategy for enhancing the electrical conductivity and mechanical adaptability owing to their extraordinary strength, electrical conductivity, and low percolation thresholds to form conductive paths[16–18] and further expand their potential for biosignal monitoring.[16,19] Nevertheless, conventional PDMS/CNT composites suffer from weak interfacial strength between CNT and PDMS substrate, arising from the great tendency of aggregation of CNT[20–22] and poor adhesion of commercial silicone (Sylgard 184).[19,23] Generally, an interface of a polymer layer is introduced to modify the CNT, increasing the adhesion with PDMS (hydrophilic treatment) and eliminating CNT detachment from the electrode substrate. However, these electrodes are not adhesive enough to tolerate the large mechanical deformations that occur in many neural activities and lack self-healing performance. Moreover, the modification process is tedious, and the interlocking polymer is mostly limited to conductive poly(3,4-ethylenedioxythiophene):poly(styrene sulfonate) (PEDOT:PSS).[8] Introducing the hydroxyl groups into the backbone of PDMS in the molecular structure can integrate both flexibility and adhesion for electrode applications. The hydroxyl groups enhance the dispersion of CNT in PDMS through the hydrogen bonds and improve adhesion to the tissue surface, offering a long-lasting functional neural interface. We prepared a block PDMS elastomer with dangling hydroxyl groups on the backbone to obtain an adhesive electrode.[24,25] However, the block PDMS suffers from low mechanical properties, leading to poor film-forming capability and weak mechanical strength for peeling.

Herein, we address these compromises by fabricating a self-healing and high-adhesive conductive electrode with crosslinked block PDMS-based elastomers doping CNT nanomaterials for chronic epilepsy monitoring. The resulting crosslinked block polyborosiloxane (C-PBS) elastomers with dangling hydroxyl groups on the backbone were synthesized through a thiol–ene click reaction. The mechanical and adhesive properties can be manipulated by the feed ratio of the component and crosslinker. This system integrates tunable mechanical properties with stiffness adjustable from 10 to over 200 kPa and meets diverse application demands. The electrode exhibits strong adhesion to both skin and neural tissues, supporting stable operation even under humid sweating conditions. Additionally, the self-healing capabilities arising from the dynamic equilibrium of the crosslinking networks enhance the durability and operational lifespan. CNTs acted as the conducting channel in the composite and endowed a low impedance, sensitive, and stable interface for the electrode. This innovative C-PBS/CNT composite offers high stretchability, high adhesion, and multichannel recording capabilities, representing a significant advancement in polymer-based biosignal interfaces and paving the way for robust, long-term solutions for epilepsy research and clinical applications.

Experimental

Materials

Vinyl-terminated polydimethylsiloxanes (v-PDMS) with a molecular weight of 8100 g mol^{-1} were purchased from J&K. Dithiothreitol (DTT) and 2,2-dimethoxy-2-phenylacetophenone (DMPA) were purchased from the Aladdin Company. Boric acid (BA) was purchased from Sinopharm Chemical Reagent Co., Ltd, sieved *via* a 100-mesh sieve aluminum screen and dried for 24 h before use. CNT (10 nm in diameter and 12 μm in length) was purchased from Soochow Tanfeng Technology. PDMS Sylgard 184 was obtained from Dow Corning. All other chemicals were analytical grade reagents and used directly without further purification.

Substrate preparation

The C-PBS elastomer was synthesized *via* a one-step thiol–ene reaction. Vinyl-terminated polydimethylsiloxane (10 g), DTT (190 mg), DMPA (32 mg), D4, and boric acid were used as precursors. The mixture was dissolved in tetrahydrofuran, purged with nitrogen for 30 minutes, and irradiated with UV light (365 nm) for 30 minutes. After removing the solvent by drying at 120 °C for 1 hour, the resulting C-PBS elastomer was collected and stored. The mechanical properties of the elastomer were optimized by varying the ratio of v-PDMS to DTT. The resulting elastomer was denoted as crosslinked C-PBS-*a*–*b* with various feed ratios and crosslinker content, where *a* represents

the feed ratio of DTT/v-PDMS and *b* represents the content of the crosslinker.

Conductive material preparation

CNTs were incorporated as conductive fillers into the C-PBS elastomer. The CNTs were dispersed with ethanol under ultrasonication to prevent aggregation and were then added to the C-PBS dispersion solution. The homogenous mixture was dried completely to obtain the conductive C-PBS/CNT composite. CNTs were added at 4%, 5%, and 6% (w/w), and their effects on conductivity and mechanical properties were evaluated. The composites were denoted as C-PBS-*a*–*b*/CNT-*i*, where *i* represents the CNT content. Excessive CNT loading increased material stiffness and reduced compatibility with the elastomer matrix, while a 4% loading provided the best balance of conductivity and flexibility.

Electrode fabrication and encapsulation

The PBS-based electrodes were fabricated by integrating conductive pathways onto the substrate using a mask-assisted technique. After patterning the C-PBS/CNT composite, the electrodes were encapsulated with a thin C-PBS layer to protect the conductive elements and enhance durability. Encapsulation also improved the adhesion of the electrodes to biological surfaces, ensuring stable and long-term contact during electrophysiological monitoring.

Mechanical properties of C-PBS/CNT composite

The mechanical properties of the C-PBS/CNT composite elastomer were evaluated using tensile and peeling tests. Tensile tests were performed on samples measuring 15 mm × 5 mm × 1 mm using a universal testing machine (CMT-4304-QY) at a strain rate of 20 mm min^{-1}. Peeling strength was measured using a 90-degree peeling test (ASTM D6862) at a peeling rate of 300 mm min^{-1} after a 5 minute dwell time. The C-PBS/CNT composite demonstrated the highest adhesion strength on the skull substrate. The self-healing ability was evaluated by testing mechanical recovery at 15 min, 30 min, 45 min, and 60 min after cutting.

Electrical property testing

The electrical properties of the C-PBS were analyzed using a Keysight E980AL Precision LCR Meter. Resistance and impedance characterizations were conducted under static and dynamic conditions, including stretching and twisting. Stretching tests were performed at a strain rate of 20 mm min^{-1} while twisting tests involved manually rotating the samples by 180°. The resistance recovered to its original value in both cases, demonstrating excellent electrical stability and self-healing capability.

Application in epileptic signal monitoring

All animal experiments performed on mice were approved by the Institutional Animal Care and Use Committee at Fudan University. Wild-type mice (WT, C57 BL6/J) were obtained from Beijing Vital River Laboratory Animal Technology Co., Ltd. The C-PBS/CNT electrodes were tested for their ability to monitor cortical epilepsy signals *in vivo*. EEG signals were recorded in mice under different states, including normal, anesthetized, and epileptic conditions. The electrodes adhered stably to the mouse skull without additional adhesives and provided continuous and reliable signal acquisition even during motion. Multi-channel recordings captured the temporal and spatial propagation of epileptic signals, highlighting the potential of C-PBS electrodes for chronic electrophysiological monitoring in both preclinical and clinical applications.

Results and discussion

Material design and characterization

Fig. 1a illustrates the synthetic process of self-healing C-PBS elastomers *via* a straightforward one-step reaction. This process involves two key chemical reactions: (1) the polymerization of vinyl-terminated PDMS (v-PDMS), dithiothreitol (DTT), and 2,4,6,8-tetramethyltetravinylcyclotetrasiloxane (D4) through thiol–ene reaction, and (2) the condensation between boronic acid (BA) and hydroxyl groups (–OH) from the DTT units incorporated into the polymer chain. The above two reactions synchronously and independently occurred during the synthetic process. Moreover, D4 serves as a crosslinker to further manipulate the mechanical properties of the elastomers. These reactions result in a robust polymer network with multiple interactive sites after solvent removal. The hydroxyl groups on the PBS backbone are favorable for adhesion and further crosslinking with BA. The resulting elastomer is denoted as crosslinked PBS (C-PBS-*a*–*b*) with dynamic and persistent covalent networks. Meanwhile, the elastomer without the addition of the D4 crosslinker is denoted as block PBS.[24] The formed dynamic boronate ester bonds enhance the mechanical and self-healing properties in combination with the hydrogen bonds among the dangling hydroxyl groups within the network. Owing to the high mobility of the PDMS chains and dynamic interactions, the elastomer demonstrates rapid and efficient self-repair upon damage, as shown in Fig. 1b. This intrinsic self-healing property highlights the potential of the synthesized C-PBS elastomer for applications requiring durability and reusability.

The chemical structure of the elastomer was first characterized by Fourier Transform Infrared (FTIR) measurement. Fig. 2a presents the FTIR spectra of v-PDMS, DTT, D4, the premixture, and the final C-PBS. The disappearance of the C=C stretching vibration (1610 cm^{-1}) from v-PDMS and D4, along with the disappearance of the –SH stretching vibration (2549 cm^{-1}) from DTT after the thiol–ene reaction,[24] confirms the near-complete consumption of functional groups during polymerization and formation of the block PBS with dangling hydroxyl groups and crosslinking network with cyclotetrasiloxane as a crosslinking point. Additionally, the broad peak at 3450 cm^{-1} is assigned to the hydroxyl group, and its intensity became weak after forming the dynamic network with BA.

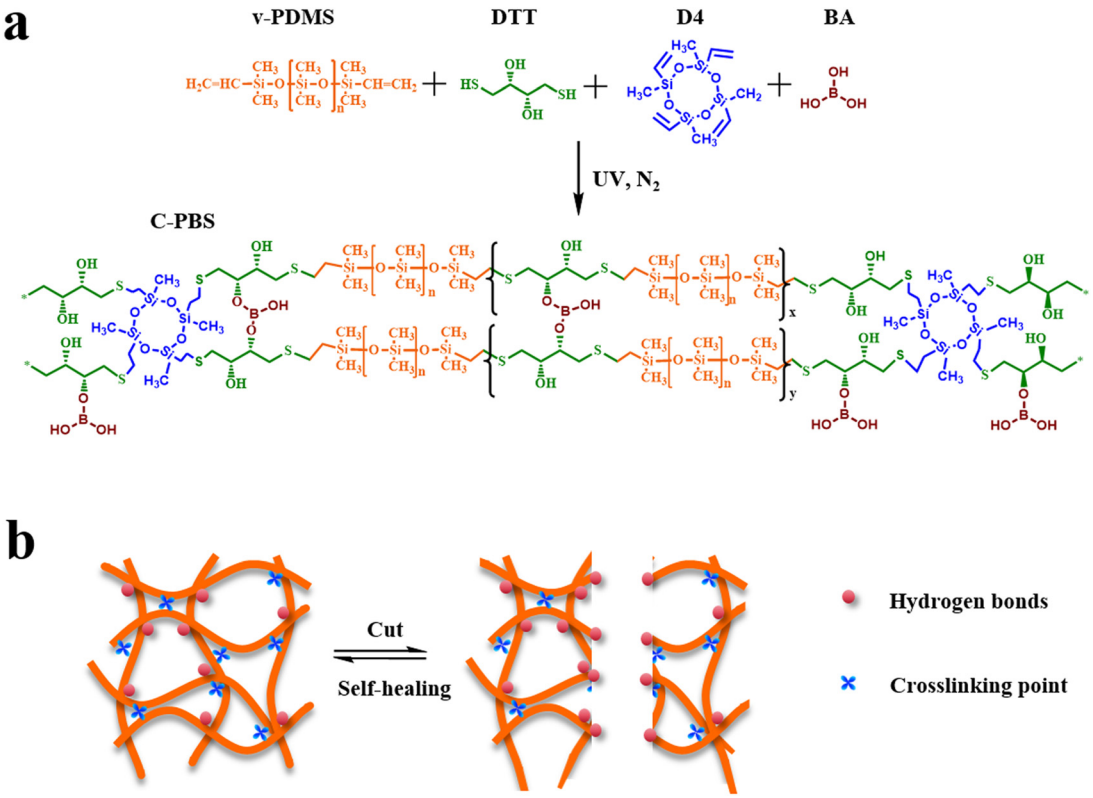

Fig. 1 Schematic of the synthesis and self-healing mechanism of C-PBS. (a) Synthetic route and chemical structure of C-PBS. (b) Types of crosslinking points in C-PBS and the self-healing mechanism.

These results demonstrate the formation of dynamic boronate ester bonds in the elastomer, further supporting the structural formation of C-PBS. The progression of the reaction can also be monitored by observing the modulus variation. Before the reaction, the premixture exists in a liquid state without shape, while the final C-PBS demonstrates notable shape manufacturability and stretchability. Mechanical testing of the C-PBS samples reveals that the tensile strength can be tailored by adjusting the feed ratio of v-PDMS to DTT. Remarkably, the material exhibits an elongation at break exceeding 1000%, as shown in Fig. 2b. Moreover, the incorporation of D4 enhances the tensile strength of C-PBS, and this effect is particularly pronounced in samples prepared with a reaction ratio of 1 : 1.2 for v-PDMS to DTT. This phenomenon is likely owing to the increased interaction between PBS chains and D4, where the external thiol groups can react with more double bonds, forming a covalent network with high density. Furthermore, the influence of crosslinker content on the mechanical properties was explored, as shown in Fig. 2c and d. The mechanical strength gradually increases with an increase in D4 content, accompanied by a decrease in elongation. This can be attributed to the high crosslinking density with more D4 crosslinkers. These results corroborate the schematic illustration in Fig. 1, confirming the successful synthesis of the C-PBS elastomer. Based on these results, a feed ratio of 1 : 1.2 is selected for further investigation of the elastomer composite, as it provides an optimal balance of mechanical properties and dispersibility for further introduction of nanofillers.

Self-healing performance and long-term stability under dynamic conditions

CNT has been widely used as a conductive filler owing to its extraordinary strength and electrical conductivity as well as its one-dimensional structure. To enhance the electrical properties of the C-PBS elastomers, CNT was chosen as the conductive media for the electrode. CNT powders were first dispersed in a solvent with ultrasonication and then mixed with C-PBS dispersion under stirring. The dispersed CNT penetrates the PBS network, forming a homogeneous nanocomposite after drying. The hydrogen bonds between the hydroxyl groups of C-PBS and the CNT surface could prevent the further aggregation of CNT with polymer chains attached to the surface.[26] Therefore, the CNT could enhance the mechanical strength and construct a continuous conducting channel with low percolation thresholds of the composite elastomer (denoted by C-PBS/CNT-*i*).[27]

The mechanical properties of the C-PBS/CNT composites were regulated by CNT contents and the D4 crosslinker, as shown in Fig. 3a and b. The resulting conductive composite elastomers carrying dynamic networks exhibited a wide range of tensile stress from 30 kPa to 230 kPa by controlling the CNT contents, as shown in Fig. 3a. Meanwhile, the addition of D4

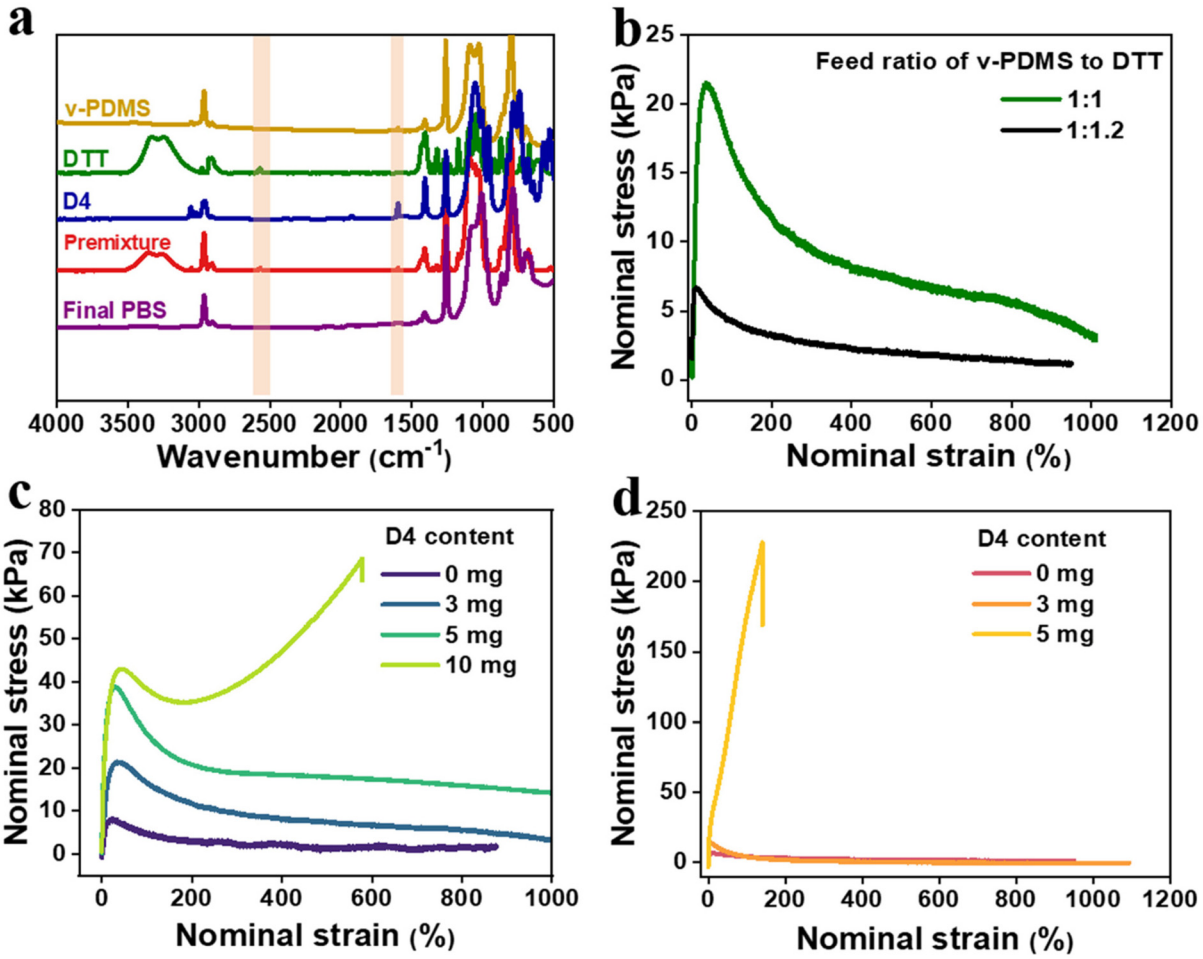

Fig. 2 Synthesis and mechanical tests of C-PBS. (a) FTIR spectra of v-PDMS, DTT, premixture of v-PDMS and DTT, block PDMS, and C-PBS. (b) Stress–strain curves of block PBS prepared with different feed ratios at 25 °C (50 mm min^{-1}). (c) Stress–strain curves of C-PBS-1-*b* (feed ratio of 1 : 1) prepared with different D4 contents at 25 °C (50 mm min^{-1}). (d) Stress–strain curves of C-PBS-1.2-*b* (feed ratio of 1 : 1.2) prepared with different D4 contents at 25 °C (50 mm min^{-1}).

further increased the tensile stress of C-PBS-1.2–3/CNT, indicating that the crosslinking density and mechanical properties could be further tuned by manipulating the formulation, which is consistent with the aforementioned results. The abundant hydrogen bonding in C-PBS also imparts unique self-adhesiveness to various substrates, enabling stable and durable interfaces for electrodes. Peeling apart materials is an important technique for characterizing adhesion properties. The peeling strength of C-PBS-1.2 prepared with different D4 amounts was quantified on the skull (Fig. S1†), as shown in Fig. 3c. The peeling strength between C-PBS-1.2 and the skull reached as high as 250 N m^{-1}, whereas Scotch tape exhibited no adhesion to the skull. It is noteworthy that the adhesion property is lower with the addition of CNT because it blocks the contact of hydroxyl groups with the surface, as shown in Fig. 3d. Considering the service conditions of flexible electrodes with softness and high adhesion, we chose C-PBS-1.2–3 with dynamic boronate ester bonds as the polymer matrix for preparing conductive electrode (C-PBS-1.2–3/CNT-4) with the addition of 4 mg CNT.

Owing to the mobility of PBS chains as well as the abundant hydrogen bonds and boronate ester bonds within the polymer matrix, C-PBS demonstrated exceptional intrinsic self-healing capabilities.[24] To quantify this spontaneous healing behavior, stress–strain curves of C-PBS-1.2–3/CNT-4 composite at various healing times were recorded, as shown in Fig. 3e. Mechanical healing efficiency can be calculated as the ratio of the restored stress to its original stress.[28] The stress gradually recovers to a high efficiency of 92% at room temperature, highlighting the ability of the composite to recover its mechanical properties after suffering cracks or fractures. Conductivity is another important feature for evaluating the capability of electrodes, and lower contact impedance is necessary to obtain high-quality signals. To further investigate the autonomous self-healing ability of the C-PBS/CNT electrode, the self-healing of electrical properties of conductive C-PBS/CNT was further

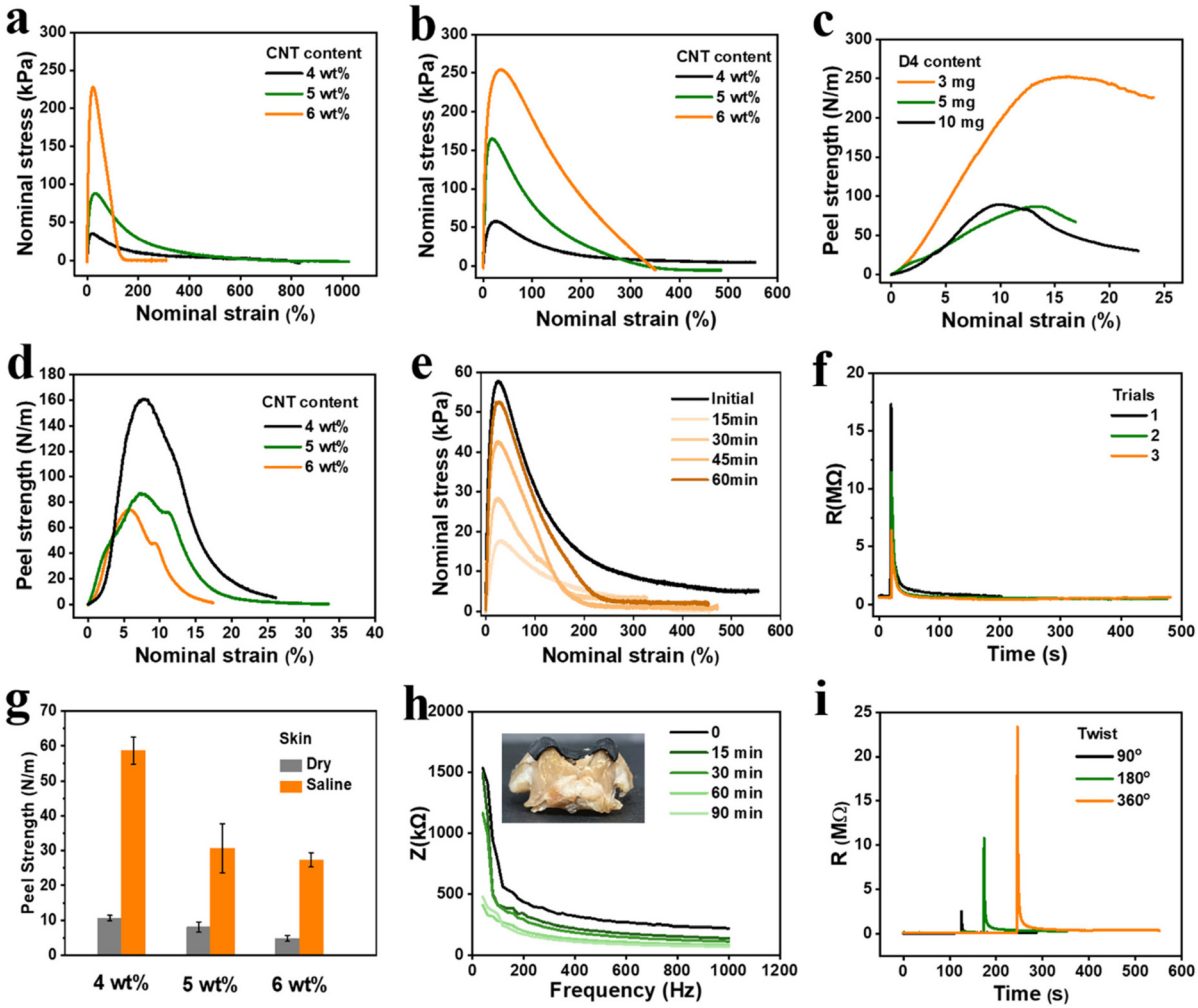

Fig. 3 Stress–strain curves of conductive (a) block PBS without D4 and (b) C-PBS-1.2–3 elastomers with different CNT contents as conductive fillers. Peeling strength of (c) C-PBS-1.2-*b* with different D4 amounts, and (d) C-PBS-1.2–3/CNT-*i* composite with different CNT contents on skull substrates. (e) Stress–strain curves of C-PBS-1.2–3/CNT-4 composite before and after self-healing, quantifying the self-healing efficiency. (f) Resistance recovery of conductive C-PBS-1.2–3/CNT-4 composite after multiple cutting and healing cycles, demonstrating consistent restoration of electrical properties. (g) Comparison of the adhesion strength of C-PBS-1.2–3/CNT-4 composite on tissue under wet and dry conditions. (h) Long-term impedance monitoring of C-PBS-1.2–3/CNT-4 composite in the test frequency range for different times. The inset shows the conformal contact between the composite and the complex curved surface. (i) Resistance recovery of C-PBS-1.2–3/CNT-4 composite after twisting, indicating stability under dynamic mechanical conditions.

evaluated by *in situ* monitoring of its resistance. When the elastomer material was cut with a razor blade, the circuit was interrupted, resulting in resistance instantly increasing to the megaohm range (Fig. 3f). Remarkably, within only 2 seconds, the resistance returned to its original value without any external stimulus. Resistance was also recorded after multiple cutting and healing cycles, demonstrating consistent recovery (Fig. 3f). This rapid and complete restoration of electrical conductivity is attributed to the autonomous reconstruction of the conductive network induced by the hydrogen bonding interactions, dynamic boronate ester bonds, and dynamic movement of the polymer chains.[28,29] Compared to previously reported self-healing electrodes, which often fail to fully recover conductivity or require an extended time for healing, the conductive C-PBS/CNT in this study offers a significant improvement. The dynamic nature of the network within the C-PBS matrix not only facilitates the reconstruction of the network for mechanical properties but also ensures efficient reconnection and transport of the conducting network for conductivity after cutting. This unique combination of abundant hydrogen bonding and CNT dispersion enables the rapid and robust recovery of both mechanical and electrical properties, making conductive C-PBS/CNT a promising electrode candidate for self-healing electronic applications.

As the electrode is applied to long-term adhesion and even sweating scenes, the peeling test of C-PBS/CNT was characterized under saline conditions to simulate the actual application scenario of the human body, as shown in Fig. 3g. The elec-

trode exhibits a high peel strength of 60 N m^{-1} on tissue under dry conditions, and the strength gradually decreases as the CNT content increases, for example, from 60 N m^{-1} with 4 mg to about 30 N m^{-1} with 6 mg CNT. This can be attributed to the fact that the presence of CNT blocks the bonding interaction with the adherends.[30] Moreover, even after soaking in saline, the C-PBS-1.2–3/CNT-4 composite maintained a peeling strength of 10 N m^{-1} on tissue, outperforming many reported underwater adhesives and even exceeding the adhesion strength of Scotch tape in air. It is commonly believed that PBS may hydrolyze in aqueous environments,[31] leading to adhesion failure. However, in this study, the D4 in the C-PBS matrix provides robust chemical crosslinking, which mitigates hydrolysis and ensures stable adhesion under wet conditions. This self-adhesiveness allows for stable and tight contact of soft electronics with interfaces, such as skin, skull, and even complex curved surfaces, as shown in Fig. S2.† Robust adhesion even after prolonged soaking in saline ensures long-term durability in wet environments, including activities in bathing or implantable applications. To further evaluate its performance under dynamic conditions, we conducted tests involving long-term impedance monitoring (Fig. 3h) and twisting (Fig. 3i). The C-PBS/CNT-4 composite demonstrates a decreasing impedance with adhesion time, which can be as low as 62 kΩ. A similar trend can be observed for the C-PBS/CNT-6 composite, as shown in Fig. S3.† Furthermore, the contact impedance gradually decreases with duration time in the test frequency range under dry conditions. This can be attributed to the dynamic C-PBS and CNT networks, resulting in closer contact and lower contact impedance for a longer time. However, compared with commercial electrodes, it shows an upward trend over time (Fig. S4†). This is related to the conduction principle of commercial electrodes. The loss of water in the hydrogel leads to an increase in impedance. Therefore, C-PBS/CNT composites with low impedance, high adhesion, and self-healing properties are suitable for bioelectronic applications that require stable and durable interfaces. After twisting at different angles, the resistance of the C-PBS/CNT composite quickly returned to its original state, demonstrating its excellent resistance to dynamic stresses. This is a critical property for applications in dynamic environments.

The biocompatibility of C-PBS/CNT was also evaluated to extend the service life and ensure safety, as it is indispensable for on-skin devices; PDMS with biocompatibility as a control sample has been well documented.[32] The C-PBS/CNT composites could adhere to the skin of C57 mice for 2 months to explore the irritation without bandages (Fig. S5†). The hematoxylin–eosin staining skin samples underneath the C-PBS/CNT composites showed no more inflammatory cell infiltration compared with normal skin nearby, further confirming the excellent biocompatibility of the C-PBS/CNT composites.

Biocompatibility and *in vivo* acquisition of epileptic activity

The C-PBS/CNT composite demonstrating excellent self-adhesion, self-healing properties, stability, and biocompatibility was fabricated as a probe for electrophysiology monitoring. Chronic epilepsy monitoring requires stable, long-term interfaces capable of conforming to dynamic, irregular biological surfaces. Conventional rigid or non-conformable flexible electronics often face issues such as delamination and poor adaptability, limiting their utility. In contrast, the exceptional self-adhesion and deformability of the complex surface of C-PBS/CNT electrodes effectively address these challenges. Moreover, for ECG monitoring, conventional electrodes are typically limited to flat surfaces, such as the chest. The flexible C-PBS/CNT electrodes enable conformal contact and ECG signal collection from irregular surfaces, such as human fingers, without the need for additional adhesives (Fig. S6†). This simplifies the collection process and extends its applicability to non-traditional recording sites. Compared with the signal recorded by the commercial electrode, high-resolution ECG signals from the arm of the human were captured by the C-PBS/CNT electrode, as shown in Fig. 4a. Waves with a high signal-to-noise ratio were recorded, demonstrating their potential for health monitoring and disease diagnosis.[33,34] Nevertheless, the same ECG signal obtained from conventional electrodes (Ag/AgCl) frequently shows large artifacts owing to the difficulty of maintaining stable contact during movement. Remarkably, the C-PBS/CNT electrode captures more reliable eye blink signals with higher amplitudes, as shown in Fig. 4b (n = 3), owing to its tighter contact with the skin.

The capability of the C-PBS/CNT probe to capture characteristic neural signals across stages of epilepsy was systematically explored, as shown in Fig. 4c–f. To further evaluate the capability of detecting signals during epileptic seizures, an assessment of the seizures in mice was implemented with a C-PBS/CNT electrode. This demonstrated remarkable stability during chronic epilepsy monitoring with fewer motion artifacts. Particularly, the C-PBS/CNT electrode maintains conformal contact on mouse skulls even during movement, enabling continuous EEG recordings from anesthetized to awake states (Fig. 4c and d) and during epileptic seizures (Fig. 4c–e). Fig. 4f shows the power spectral density (PSD) of mouse brain activity under anesthetized, awake, and epileptic conditions. Low-frequency dominance (0–4 Hz) is observed in the anesthetized state, while the awake state exhibits broader frequency activation with increased mid- and high-frequency power (10–50 Hz). The epileptic state shows elevated high-frequency power (30–80 Hz), reflecting abnormal neuronal synchronization. We repeated these experiments in 3 mice and obtained similar results. These acquired characteristic oscillation signals are favorable for speculating certain states of epilepsy. Nevertheless, conventional EEG systems are limited to anesthetized animals owing to the difficulty of maintaining stable contact during movement. This robust adhesion ensures the long-term reliability of C-PBS/CNT electrodes, conquering the limitations of commercial electrodes, which often fail because of their size, stiffness, and poor adaptability to dynamic environments. Therefore, the C-PBS/CNT electrode provides a versatile and reliable solution for advancing epilepsy research and improving disease management in both animal and clinical settings.

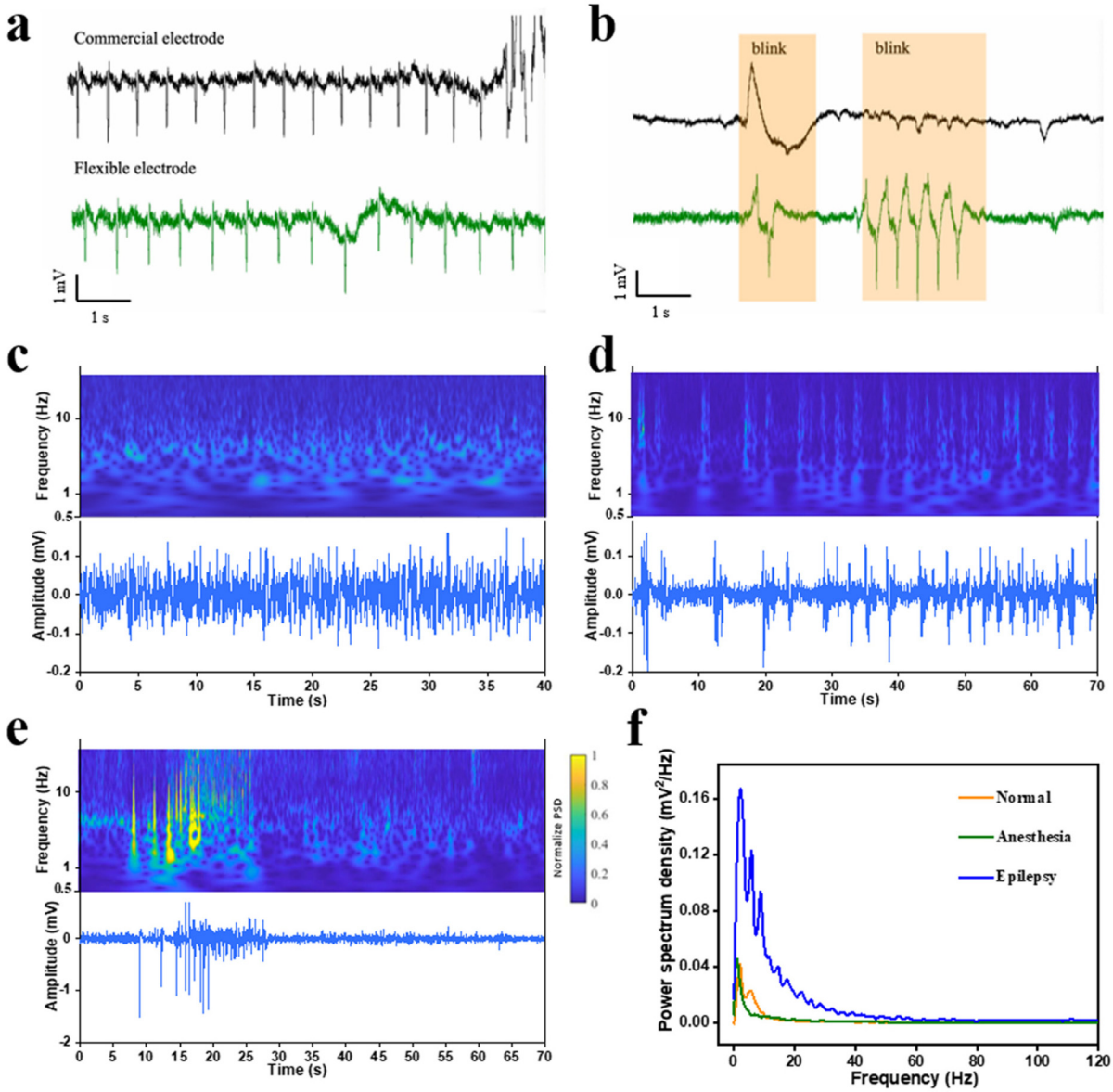

Fig. 4 (a) ECG and (b) EEG signals collected with commercial electrodes and C-PBS/CNT flexible electrodes attached to the human skin. Example *in vivo* EEG recordings with flexible electrodes attached to the skin above the skull of an epileptic mouse in (c) the normal awake state and (d) anesthetized state, and (e) the onset and cessation of an event of epileptic seizure. (f) Power spectrum density of these different states.

Conclusion

In this study, we developed a flexible, self-healing, and highly adhesive C-PBS/CNT composite with tunable mechanical properties, self-healing, and excellent biocompatibility for advanced bioelectronic applications. The unique combination of abundant hydrogen bonds and tailored dynamic bonds endows the C-PBS with exceptional self-healing capabilities, stability in dynamic environments, and outstanding adhesion to skin and skull substrates. The mechanical properties could be manipulated by controlling the crosslinker and feed ratio. These properties enable the PBS-based electrodes to maintain conformal contact and reliable epilepsy monitoring performance with precise signal acquisition for both animal and human studies under complex and wet conditions, outperforming conventional Ag/AgCl electrodes. Their ability to capture high-quality signals during dynamic movements, including EEG monitoring in awake and epileptic mice, marks a significant advancement in chronic monitoring systems. This work provides a versatile and reliable platform for bioelectronics, expanding the scope of flexible, self-healing polymers in healthcare. The innovations presented herein open new avenues for developing next-generation wearable and implantable devices, particularly for long-term monitoring and disease diagnosis, aligning with the mission of advancing functional polymer materials for cutting-edge applications.

Author contributions

M. T., and Z. L. conceived the concept and designed the research. M. T. and K. L. conducted the material experiments. X. H. and X. Z. conducted the adhesion tests and ECG tests. Q. H. analyzed the EEG data. M. T. and Z. L. wrote the manuscript. All the authors discussed the results and commented on the manuscript.

Data availability

The data supporting this article have been included as part of the ESI.† Additional data are available upon request.

Conflicts of interest

Hualiang Ni serves as the CEO at Aoyi Information Technology Co., Ltd, but this did not influence the design or outcomes of the study. The remaining authors have no conflicts to disclose.

Acknowledgements

The authors would like to acknowledge the support from the National Natural Science Foundation of China (32300935, 32130044, T2241002, 32100930), Ministry of Science and Technology of People's Republic of China (STI2030-Major Projects 2021ZD0202500), Program of Shanghai Academic/Technology Research Leader (21XD1400100), Shanghai Rising Star Program (23YF1407200), and FDUROP (23823). Part of the experimental work was carried out in the Fudan Nano-fabrication Lab.

References

1 G. L. Fialho, T. D. Pang, W. Y. Kong, A. P. Tran, C. G. Yu, I. D. Rodriguez, B. D. Nearing, J. W. Waks, T. R. Maher and J. R. Clarke, *Epilepsia*, 2023, **64**, 2361–2372.
2 P. J. Karoly, V. R. Rao, N. M. Gregg, G. A. Worrell, C. Bernard, M. J. Cook and M. O. Baud, *Nat. Rev. Neurol.*, 2021, **17**, 267–284.
3 A. C. Paulk, P. Salami, R. Zelmann and S. S. Cash, *Neurosurg. Clin.*, 2024, **35**, 135–149.
4 G. Hong and C. M. Lieber, *Nat. Rev. Neurosci.*, 2019, **20**, 330–345.
5 K. Liu, H. Zhang, M. Hu, Z. Li, K. Xu, D. Chen, W. Cui, C. Lv, R. Ding and X. Geng, *Mater. Adv.*, 2024, **5**, 4958–4973.
6 R. Dong, L. Wang, Z. Li, J. Jiao, Y. Wu, Z. Feng, X. Wang, M. Chen, C. Cui and Y. Lu, *ACS Nano*, 2024, **18**, 1702–1713.
7 L. Yang, Q. Liu, Z. Zhang, L. Gan, Y. Zhang and J. Wu, *Adv. Mater. Technol.*, 2022, **7**, 2100612.
8 X. Li, Y. Song, G. Xiao, E. He, J. Xie, Y. Dai, Y. Xing, Y. Wang, Y. Wang and S. Xu, *ACS Appl. Bio Mater.*, 2021, **4**, 8013–8022.
9 K. Y. Lee, H. Moon, B. Kim, Y. N. Kang, J. W. Jang, H. K. Choe and S. Kim, *Adv. Mater. Interfaces*, 2020, **7**, 2001152.
10 Y. Berdichevsky, J. Khandurina, A. Guttman and Y.-H. Lo, *Sens. Actuators, B*, 2004, **97**, 402–408.
11 F. Zheng, C. He, P. Fang, J. Wang, B. Xiong, K. Wang, F. Liu, X. Peng, X. Xu and Z. Xu, *Appl. Surf. Sci.*, 2013, **283**, 327–331.
12 J. Wang, K. Wang and F. Xiao, *Nanoscale*, 2023, **15**, 9031–9039.
13 J. Zhang, Y. Chen and M. A. Brook, *Langmuir*, 2013, **29**, 12432–12442.
14 A. Shakeri, S. Khan and T. F. Didar, *Lab Chip*, 2021, **21**, 3053–3075.
15 G. Li, Z. Qiu, Y. Wang, Y. Hong, Y. Wan, J. Zhang, J. Yang, Z. Wu, W. Hong and C. F. Guo, *ACS Appl. Mater. Interfaces*, 2019, **11**, 10373–10379.
16 J. Wang, J. Yu, H. Wei, A. Wang, Z. Hou, M. Kumi, X. Wang, T. Wang, P. Li and W. Huang, *Adv. Funct. Mater.*, 2024, **34**, 2407394.
17 K. Lee, S. Mhin, H. Han, O. Kwon, W.-B. Kim, T. Song, S. Kang and K. M. Kim, *J. Mater. Chem. A*, 2022, **10**, 1299–1308.
18 Q. Li, J. Li, D. Tran, C. Luo, Y. Gao, C. Yu and F. Xuan, *J. Mater. Chem. C*, 2017, **5**, 11092–11099.
19 J. Zhang, X. Liu, W. Xu, W. Luo, M. Li, F. Chu, L. Xu, A. Cao, J. Guan and S. Tang, *Nano Lett.*, 2018, **18**, 2903–2911.
20 Z. Li, J. Peng and Z. Lin, *Giant*, 2021, **5**, 100048.
21 Z. Li, M. Tang, J. Dai, T. Wang and R. Bai, *Polymer*, 2016, **85**, 67–76.
22 Z. Li, M. Tang, W. Bai and R. Bai, *Langmuir*, 2017, **33**, 6092–6101.
23 H. Li, H. Zhao, K. Song, F. Han, Z. Liu and Q. Tian, *Nanoscale*, 2024, **16**, 6402–6428.
24 M. Tang, Z. Li, K. Wang, Y. Jiang, M. Tian, Y. Qin, Y. Gong, Z. Li and L. Wu, *J. Mater. Chem. A*, 2022, **10**, 1750–1759.
25 M. Tang, Z. Jiang, Z. Wang, Y. Qin, Y. Jiang, L. Wu and Z. Li, *Chem. Eng. J.*, 2023, **451**, 138730.
26 M. P. Wolf, G. B. Salieb-Beugelaar and P. Hunziker, *Prog. Polym. Sci.*, 2018, **83**, 97–134.
27 I. You, M. Kong and U. Jeong, *Acc. Chem. Res.*, 2018, **52**, 63–72.
28 M. Tang, P. Zheng, K. Wang, Y. Qin, Y. Jiang, Y. Cheng, Z. Li and L. Wu, *J. Mater. Chem. A*, 2019, **7**, 27278–27288.
29 D. Son, J. Kang, O. Vardoulis, Y. Kim, N. Matsuhisa, J. Y. Oh, J. W. To, J. Mun, T. Katsumata and Y. Liu, *Nat. Nanotechnol.*, 2018, **13**, 1057–1065.
30 M. D. Bartlett, S. W. Case, A. J. Kinloch and D. A. Dillard, *Prog. Mater. Sci.*, 2023, **137**, 101086.

31 W. Tongfei and C. Biqiong, *Ind. Eng. Chem. Res.*, 2016, **55**, 6113–6121.
32 S. H. Kim, J.-H. Moon, J. H. Kim, S. M. Jeong and S.-H. Lee, *Biomed. Eng. Lett.*, 2011, **1**, 199–203.
33 A. Kolanowska, A. P. Herman, R. G. Jędrysiak and S. Boncel, *RSC Adv.*, 2021, **11**, 3020–3042.
34 A. C. Myers, H. Huang and Y. Zhu, *RSC Adv.*, 2015, **5**, 11627–11632.